

# Ultra-Peripheral Collisions in PHENIX

Zaida Conesa del Valle, for the PHENIX Collaboration

Laboratoire Leprince-Ringuet, Ecole Polytechnique - CNRS/IN2P3, Palaiseau, France

Ultra-peripheral nuclei collisions provide means to study photon-induced interactions in a nuclear environment. We discuss the PHENIX collaboration results on  $J/\psi$  and  $e^+e^-$  photoproduction in Au+Au ultra-peripheral collisions at  $\sqrt{s_{NN}} = 200$  GeV [1, 2]. Their production cross-section and transverse momentum spectra are presented. The results are compared and found to be consistent with various theoretical calculations.

## 1 Motivation

High energy particle collisions are the experimental tools to improve our understanding of the elementary particles and their interactions [1]. Photon-induced reactions are an interesting approach to study strong and electromagnetic interactions, complementarily to  $e^+e^-$ ,  $ep$  (DIS),  $pp$  and  $p\bar{p}$  collisions. Traditionally,  $\gamma\gamma$  and  $\gamma p$  interactions have been studied in fixed target experiments with electron beams (e.g. PEP, LEP), in  $e^+e^-$  colliders, and with the HERA electron-proton collider. Recently, the photon fluxes generated at proton or nuclei collisions have attained a large enough luminosity to open the possibility to study  $\gamma\gamma$ ,  $\gamma n$  (photon-nucleon) and  $\gamma A$  (photon-nuclear) interactions as well. See Fig. 1 (left) for a comparison of the equivalent photon luminosities at various colliders [3]. These studies become experimentally possible in the ultra-peripheral collisions (UPC). UPC are protons or nuclei reactions where the impact parameter is larger than twice the nuclear radius such as there is no strong interaction. The main advantages of hadron vs. lepton colliders are the larger photon luminosity (the photon spectrum is proportional to  $Z^2$ , the two-photon luminosity goes as  $Z^4$ ) and the opportunity to probe strong electromagnetic fields (coupling  $\propto Z\sqrt{\alpha}$  instead of  $\propto \sqrt{\alpha}$ ).

The ultra-peripheral Au+Au collisions at  $\sqrt{s_{NN}} = 200$  GeV are possible thanks to the BNL RHIC collider and give access to photon-nucleon and two-photon interactions at a maximum centre-of-mass energy of  $W_{\gamma n}^{max} \sim 34$  GeV and  $W_{\gamma\gamma}^{max} \sim 6$  GeV respectively [1]. These energies allow the study of photoproduction of dileptons and vector mesons [3]. The STAR collaboration has measured  $\rho^0$  photoproduction at RHIC [4], and this proceeding concentrates on the first measurement ever of  $J/\psi \rightarrow e^+e^-$  and high-mass  $e^+e^-$  in UPC heavy-ion collisions with the PHENIX experiment [1, 2]. Exclusive  $J/\psi$  photoproduction can proceed via Pomeron-exchange (two-gluon picture) either through coherent photon-nuclear ( $\gamma A \rightarrow J/\psi$ ) or incoherent photon-nucleon ( $\gamma n \rightarrow J/\psi$ ) reactions. The  $J/\psi$  photoproduction cross section is then related to the gluon nuclear distribution functions,  $G_A(x, Q^2)$ . This allows one to constrain them in the small Bjorken- $x$  region,  $x = m_{J/\psi}^2/W_{\gamma A}^2 \cdot e^{\pm y}$  which for  $|y| \leq 0.35$  gives  $x \sim 10^{-2}$ , a relatively unexplored region (see Fig. 1 right [5]), and to eventually probe quarkonia propagation in normal nuclear matter (the so called nuclear absorption). On the other hand, exclusive dilepton ( $e^+e^-$ ) pair production can occur through a pure electromagnetic process ( $\gamma\gamma \rightarrow e^+e^-$ ) and tests QED on a strongly interacting regime.

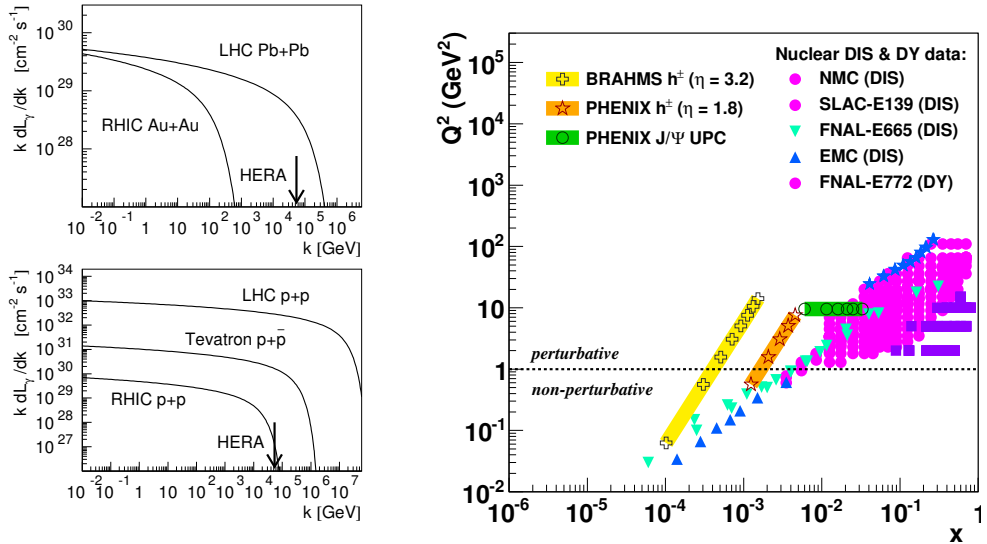


Figure 1: Left: Equivalent photon luminosity in heavy ion (top) and proton (bottom) collisions [3]. The arrow represents the maximum photon energy in HERA  $ep$  collisions. Right: Kinematic  $Q^2$  versus Bjorken- $x$  map of the regions explored to probe the nuclear PDFs [5].

## 2 The Measurement

The measurement of the ultra-peripheral probes of the interaction is experimentally challenging. Here we concentrate on the  $J/\psi \rightarrow e^+e^-$  measurement in UPC Au+Au collisions at  $\sqrt{s_{NN}} = 200$  GeV. Therefore, we examine the apparatus capabilities to detect and identify electrons and to trigger on UPC.

### 2.1 Experimental Setup

The PHENIX experiment was designed to study the most central heavy-ion collisions at the BNL RHIC collider [2]. The apparatus is formed by four spectrometers (north, south, east, west) and a few global detectors. The forward arms (north and south spectrometers,  $1.2 < |\eta| < 2.2$ ) detect and identify muons, whereas the central arms (east and west spectrometers,  $|\eta| < 0.35$ ) measure electrons, photons and hadrons. Figure 2 presents a scheme of the experimental setup as it was on year 2004 [2]. Minimum bias events are triggered with the help of the Beam-Beam Counters (BBC, at  $3.1 < |\eta| < 3.9$ ) and Zero Degree Calorimeters (ZDC, located at  $\pm 18$  m from the interaction point and covering  $|\theta| < 2$  mrad). Electron tracking and identification is possible thanks to (from inner to outer): the multi-layer drift chambers (DC), the multi-wire proportional chambers (PC), the Ring-Imaging-Cherenkov detectors (RICH) and the electromagnetic calorimeters (EMCal) with two different technologies: lead-scintillator sandwich (PbSc), and lead-glass Cherenkov (PbGl) calorimeters.

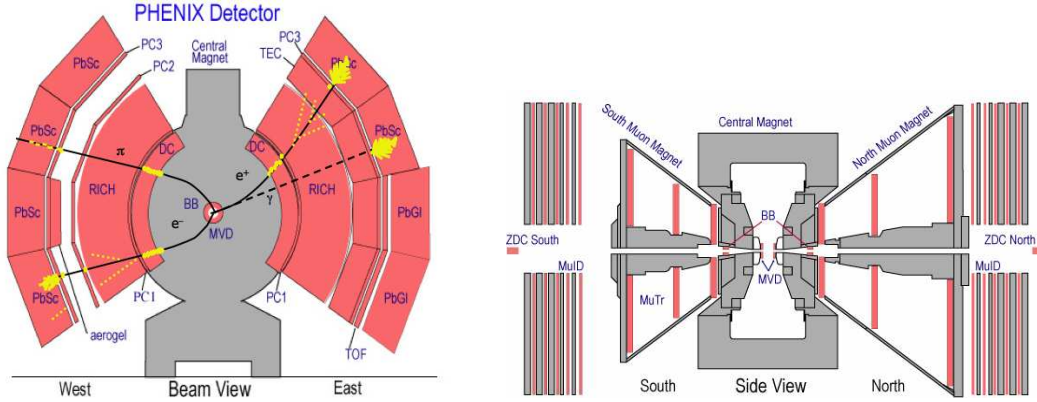


Figure 2: Section of the PHENIX central (left) and forward (right) arms as they were on year 2004 [2]. For illustration, passage of electrons, positrons, photons and pions through the central detectors are depicted.

## 2.2 Trigger Strategy

The strong electromagnetic fields associated with the ultra-relativistic heavy-ions lead to a large probability to exchange additional soft photons which can excite the interacting nuclei. The Giant-Dipole-Resonance (GDR) mechanism is the dominant excitation mode, which most probably decays by emitting neutrons at forward rapidities. The probability of  $J/\psi$  coherent production ( $\gamma A \rightarrow J/\psi$ ) in coincidence with Au Coulomb excitation leading to the emission of at least one neutron at forward rapidity is of  $55 \pm 6\%$ , whereas it is of  $\approx 100\%$  for  $J/\psi$  incoherent production ( $\gamma n \rightarrow J/\psi$ ) [6]. This characteristic has been exploited for tagging the UPC events, and, as the probability of exchanging one or several photons factorise, it does not introduce any bias on the determination of the  $J/\psi$  photoproduction cross-section. Therefore, the chosen trigger configuration was to:

1. detect these neutrons in one or both ZDC,
2. impose a veto on coincident signals on both BBCs, which selects exclusive-like events with at least one large rapidity gap and helps to reject peripheral or beam-gas interactions,
3. use an EMCAL trigger to consider events with one or more electrons of energy  $> 1$  GeV on the final state.

The efficiency of this trigger setup for  $e^+e^-$  pairs of  $m_{e^+e^-} > 2$  GeV/c<sup>2</sup> is  $90 \pm 10\%$  (see details in reference [1]).

## 2.3 Data Analysis

The total equivalent sampled luminosity by PHENIX during the 2004 RHIC Au+Au run at  $\sqrt{s_{NN}} = 200$  GeV is of  $\mathcal{L}_{integrated} = 141 \pm 12 \mu\text{b}^{-1}$ . The subsample of events analyzed correspond to those centred in the detector fiducial area (vertex in  $\pm 30$  cm) and with only two charged particles (electrons) in the final state. This is a restrictive criteria to identify

exclusive processes characterised by a few isolated particles. Electron identification criteria are enumerated in reference [1].

A total of 28  $e^+e^-$  pairs and zero like-sign pairs ( $e^+e^+ + e^-e^-$ ) with  $m_{ee} > 2$  GeV/c<sup>2</sup> have been measured (Fig. 3 left). The continuum and  $J/\psi$  components are isolated by fitting the invariant mass spectra with a continuum (exponential) plus a  $J/\psi$  (Gaussian) shape:

$$\frac{dN}{dm_{e^+e^-}} = \frac{A}{\sqrt{2\pi} \cdot \sigma} \cdot e^{-(m_{e^+e^-} - \mu)^2 / (2\sigma^2)} + C \cdot e^{B m_{e^+e^-}},$$

where  $A$ ,  $\sigma$  &  $\mu$  are the yield, width and mean position of the  $J/\psi$  peak, and  $C$  &  $B$  are the continuum normalization and slope respectively. Despite the poor statistics, the trend is compatible with STARLIGHT [6] MonteCarlo simulations and a full reconstruction with our experimental setup. The choice of the fit functional form is justified by these simulations. The number of  $J/\psi$  is of  $N[J/\psi] = 9.9 \pm 4.1(\text{stat}) \pm 1.0(\text{syst})$ , and of continuum  $e^+e^-$  counts  $N[e^+e^-] = 13.7 \pm 3.7(\text{stat}) \pm 1.0(\text{syst})$  for  $m_{ee} \in [2.0, 2.8]$  GeV/c<sup>2</sup>. The quoted systematical uncertainties consider variations of the fit function; we also test a continuum power law form and study the dependence on the slope parameters. The statistical and systematical uncertainties on the  $e^+e^-$  continuum contribution to the invariant mass distribution are represented by dashed-lines in Fig. 3 left. After correcting for the limited experimental acceptance and by the inefficiencies, we compute the doubly differential dielectron photoproduction cross-sections per invariant mass range (see Tab. 1), and the  $J/\psi$  differential photoproduction cross section at mid-rapidity ( $|\eta| < 0.35$ ), which is:

$$\frac{d\sigma_{J/\psi+Xn}}{dy} = 76 \pm 31(\text{stat}) \pm 15(\text{syst}) \text{ } \mu\text{b}.$$

Remark that all these cross-sections calculations correspond to particle production in coincidence with forward neutron emission (labelled as “ $+Xn$ ”). In addition, the pairs transverse momentum ( $p_T$ ) distribution is shown in Fig. 3 (right) as a function of their invariant mass.

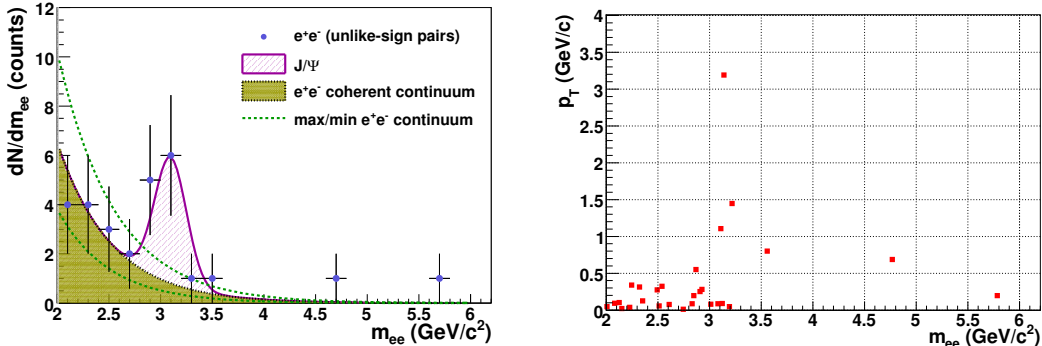


Figure 3:  $e^+e^-$  invariant mass distribution as measured in Au+Au UPC at  $\sqrt{s_{NN}} = 200$  GeV with PHENIX. The left plot depicts its decomposition into continuum and  $J/\psi$ . The right figure presents the invariant mass versus pair  $p_T$  correlation.

$m_{e^+e^-}$ [GeV/c <sup>2</sup> ]	$d^2\sigma/dm_{e^+e^-}dy _{y=0}$ [ $\mu\text{b}/(\text{GeV}/\text{c}^2)$ ]	
	DATA	STARLIGHT
[2.0, 2.8]	$86 \pm 23$ (stat) $\pm 16$ (syst)	90
[2.0, 2.3]	$129 \pm 47$ (stat) $\pm 28$ (syst)	138
[2.3, 2.8]	$60 \pm 24$ (stat) $\pm 14$ (syst)	61

Table 1: Measured  $e^+e^-$  continuum photoproduction cross sections at mid-rapidity in UPC Au+Au collisions (accompanied with forward neutron emission) at  $\sqrt{s_{NN}} = 200$  GeV. For comparison, the STARLIGHT predictions are also quoted [6].

### 3 Results Interpretation

The dielectron pairs (of  $m_{e^+e^-} \in [2.0, 2.8]$  GeV/c<sup>2</sup>) low transverse momentum (see Fig. 3 right), and their doubly differential photoproduction cross section (see Tab. 1), are in good agreement with the STARLIGHT calculations [6] for coherent ( $\gamma\gamma \rightarrow e^+e^-$ ) photoproduction accompanied with forward neutron emission ( $e^+e^- + Xn$ ). Consequently, the measurements are in agreement with LO QED theoretical calculations (STARLIGHT) even in this strongly interacting regime. Further conclusions are limited by, on the one hand, the poor statistics (the measurement uncertainties), and, on the other hand, by the deficit of other theoretical calculations in the kinematic regime of interest, and the lack of knowledge of the higher order QED contributions [7, 8].

The  $J/\psi$   $p_T$  distribution (Fig. 3 right) suggests the presence of both coherent ( $\gamma A$ ) and incoherent ( $\gamma n$ ) contributions, consistent with low and intermediate to high  $p_T$  respectively, and in agreement with the theoretical expectations [9]. The  $J/\psi + Xn$  photoproduction cross-section is compared in Fig. 4 and Fig. 5 to various theoretical calculations. Note that the predictions for both coherent and incoherent contributions are drawn separately (Fig. 4 left) and, whenever possible, also summed up (Fig. 4 right). Besides, Fig. 5 illustrates the sensitivity of the coherent  $J/\psi$  production as computed by [12] to different shadowing schemes. The predictions of references [9, 11, 12] have been scaled down according to [6] to account for the cross-section reduction when requiring forward neutron emission. The measurement is thus consistent with different model calculations even though the current precision precludes yet any detailed conclusion on the basic ingredients: shadowing and nuclear absorption.

Finally, one can also compare to HERA  $ep$  data of  $J/\psi$  photoproduction. A rough comparison is possible dividing the production cross-sections by the equivalent (theoretical) photon spectrum ( $dN/d\omega$ ) [6]:

$$\begin{aligned} \sigma_{\gamma A \rightarrow J/\psi A} &= \frac{d\sigma_{AA \rightarrow J/\psi AA}}{dy} \cdot \frac{1}{2 dN/d\omega} ; \\ \sigma_{\gamma A \rightarrow J/\psi A} &\approx A^\alpha \sigma_{\gamma p \rightarrow J/\psi p} . \end{aligned}$$

The equivalent photon spectrum at midrapidity for  $\langle W_{\gamma p} \rangle = 24$  GeV is  $2 dN/d\omega = 6.7$  (10.5) for coherent (incoherent)  $J/\psi$  production [6]. At HERA,  $\sigma_{\gamma p \rightarrow J/\psi p} = 30.5 \pm 2.7$  nb at  $\langle W_{\gamma p} \rangle = 24$  GeV [13]. If we assume, for the sake of simplicity, that the coherent and incoherent contributions to  $J/\psi$  are of 50%-50%, we obtain that the scaling with the number of nucleons ( $A$ ) is:  $\alpha_{coh} = 1.01 \pm 0.07$  for the coherent and  $\alpha_{incoh} = 0.92 \pm 0.08$  for the incoherent components respectively. This is consistent with the naive expectation of a scaling with the number of

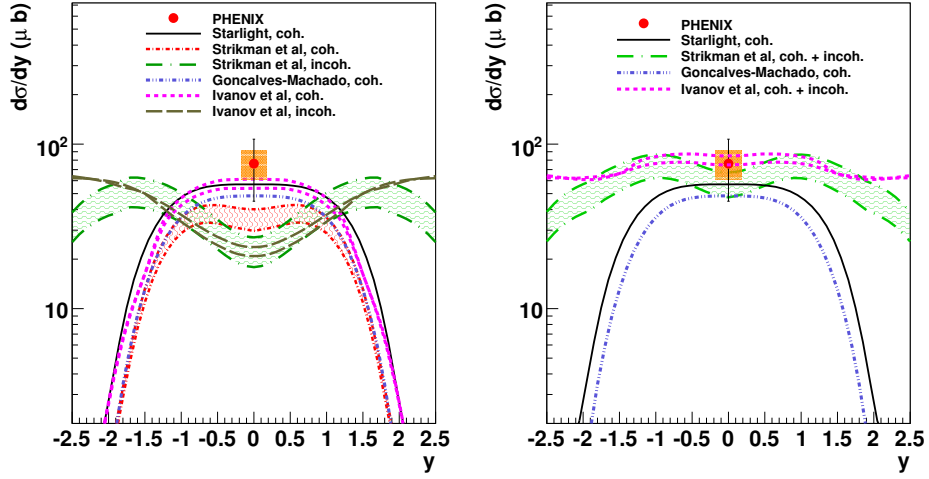


Figure 4: Comparison of the measured  $J/\psi + Xn$  photoproduction cross section with various theoretical calculations. Some of them include both coherent and incoherent components (labelled as “coh. + incoh.”) : Strikman *et al* [9], Ivanov *et al* [11]. The rest only compute the coherent contribution: STARLIGHT [6], Gonçalves *et al* [10].

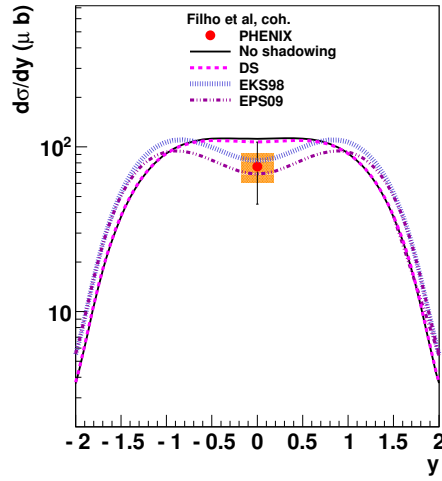


Figure 5: Comparison of the measured  $J/\psi + Xn$  photoproduction cross section with the theoretical calculations of the coherent contribution from Filho *et al* [12] with respect to different shadowing parameterisations.

colliding nucleons of the photonuclear cross-section for hard probes.

## 4 Summary

The PHENIX experiment has proven its versatility by presenting the first measurement ever of high-mass  $e^+e^-$  and  $J/\psi$  photoproduction in ultra-peripheral heavy-ion reactions [1] in Au+Au collisions at  $\sqrt{s_{NN}} = 200$  GeV (accompanied by Au Coulomb nuclear breakup). Dielectron photoproduction cross sections are in agreement with theoretical STARLIGHT LO QED calculations for coherent two-photon production,  $\gamma\gamma \rightarrow e^+e^-$ .  $J/\psi$  photoproduction cross section and its  $p_T$  pattern are consistent with the expectations [6, 9, 10, 11, 12] and favour the possibility of both coherent ( $\gamma A \rightarrow J/\psi$ ) and incoherent ( $\gamma n \rightarrow J/\psi$ ) contributions. Even though the poor statistics prevents one from ruling out any hypothesis, it shows itself to be a promising tool to learn about  $J/\psi$  production processes and probe the gluon nuclear PDFs at low- $x$ . Future analysis at RHIC with higher luminosities and the imminent LHC collisions will provide more discriminating tools.

## References

- [1] PHENIX Collaboration, A. Afanasiev et al, *Phys. Lett.* **B679**, 321 (2009) , and references therein.
- [2] PHENIX Collaboration, K. Adcox et al, *Nucl. Instrum. Meth.* **A449** (2003) 469-479.
- [3] J. Nystrand, *Nucl. Phys.* **A787** 29 (2007); *Nucl. Phys.* **A752** 470-479 (2005).
- [4] STAR Collaboration, B.I. Abelev et al, *Phys. Rev.* **C77** (2008) 034910; C. Adler et al, *Phys. Rev. Lett.* **89** (2002) 272302.
- [5] D. d'Enterria, *Nucl. Phys. Proc. Suppl.* 184:158-162 (2008), *arXiv*: 0711.1123 (2007).
- [6] A.J. Baltz, S.R. Klein and J. Nystrand, *Phys. Rev. Lett.* **89** 012301 (2002); S.R. Klein and J. Nystrand, *Phys. Rev.* **C60** 014903 (1999); A.J. Baltz, Y. Gorbunov, S.R. Klein, and J. Nystrand, *Phys. Rev.* **C80** 044902 (2009).
- [7] A.J. Baltz, *Phys. Rev. Lett.* **100** 062302 (2008).
- [8] U.D. Jentschura and V. G. Serbo, *arXiv:0908.3853*, to appear in *Eur. Phys. J. C*.
- [9] M. Strikman, M. Tverskoy, M. Zhalov, *Phys. Lett.* **B626** (2005) 72-79.
- [10] V.P. Gonçalves and M.V.T. Machado, *arXiv:0706.2810* (2007); *J. Phys.* **G32**:295-308 (2006).
- [11] Y.P. Ivanov, B.Z. Kopeliovich, I. Schmidt, *arXiv:0706.1532* (2007).
- [12] A.L. Ayala Filho, V.P. Gonçalves and M.T. Griep, *Phys. Rev.* **C78**, 044904 (2008).
- [13] ZEUS Collaboration, S. Chekanov et al, *Eur. Phys. J. C* **24** (2002) 345; H1 Collaboration, A. Aktas et al, *Eur. Phys. J. C* **46** (2006) 585.